

CHAPTER 8. PETROLOGICAL STUDIES OF CALC-SILICATE ROCKS FROM OTHER PARTS OF THE SAMB

8.1 Introduction

The calc-silicate rocks belonging to the ‘Southern Aravalli Mountain Belt’ (SAMB) also occur within the Champaner Group mainly, apart from the Lunavada Group lying within the Gujarat state. Comparative studies of calc-silicate rocks from Lunavada Group with those from Champaner Group were carried out with respect to their petrogenesis. For this purpose field studies were carried out in and around villages, viz. Wadek, Chalvad, Vav, Gandhra, Poyeli, Ambapani, Jothvad (Goldungari) and Nanikhatva located within the Champaner Group. Field work was also carried out around Chhota Udepur area, SAMB, which revealed that only dolomitic rocks occur in this region and the presence of calc-silicate rocks is lacking. Hence the rocks from this area are out of the scope of present study.

The Champaner Group is geographically located at the south-western part of Lunavada Group. Both the groups are partitioned by Godhra granite. The Champaner group is also considered as a major Proterozoic stratigraphic unit of the Southern Aravalli Mountain Belt (SAMB) in Gujarat (Fig.8.1). It was previously termed as “Champaner Series” by (Blanford, 1869) and is considered as a part of the upper Aravalli supracrustal rocks which are exposed at the eastern most periphery of Gujarat, India.

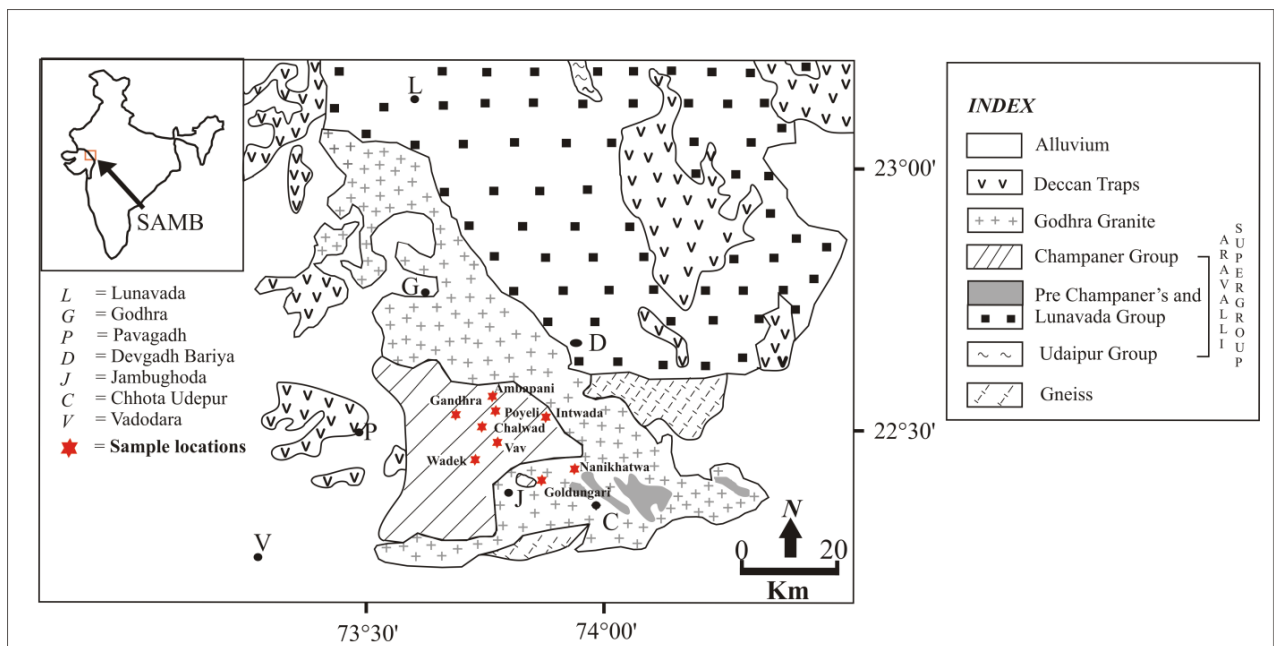


Figure 8.1: Calc-silicate sample locations within the Champaner Group, SAMB, Gujarat (modified after Gupta et al.,1992).

8.2 Background information

Uptill now in this area considerable work with respect to stratigraphy has been carried out by (Blandford,1869; Fermor,1909; Hobson,1926; RamaRao,1931; Gupta and Mukherjee,1938; Rasul,1965; Sadashivaiah and Tenginakai,1966; Jambusaria and Merh, 1967; Bhaskar Rao and Emile,1968; Yellur,1969; Jambusariya,1970; Gopinath et al.,1977; Shah et al.,1984; Gupta et al.,1992; Merh,1995; Srikarni and Das,1996; Karanth and Das,2000; Das,2003; Das et al.,2009; Sahu,2012; Sharma and Golani,2013) and with respect to structural aspects by Joshi (2019) and as the calc-silicates present here remained uninvestigated, they have been studied in terms of petrography, mineral chemistry, geochemistry as well as their metamorphic conditions in the present work to understand their petrogenesis.

8.3 Geological set-up

The Champaner Group is considered to be the youngest group in the Aravalli Supergroup. It has been divided into six formations, viz. Lambia, Khandia, Narukot, Jaban, Shivrajpur and Rajgarh formations from oldest to youngest (Gupta et al., 1992) and the 'calc-silicate rocks of this group reside within the 'Khandia Formation' (Srikarni and Das, 1996),(Fig 8.2).

The Godhra granite intrudes the Champaner group also and its exposures can be seen on the north, east and south borders of the Champaner Group. The Champaner Group possesses cyclic sequence of phyllite, quartzite and meta-conglomerate intercalated with minor-to-major bands of dolomitic limestone.

It had experienced three episodes of deformation, viz. D₁, D₂ and D₃, which have developed F₁, F₂ and F₃ folds respectively. The first two phases of deformation are coaxial, to develop F₁ with ~ ESE-WNW and F₂ with ~ E-W trending folds. The third episode of deformation exhibits fold trends ranging from NNW-SSE to NNE-SSW (Joshi, 2019).

Field studies have shown that the calc-silicates present in the area around Champaner are fine to medium grained and light grey coloured generally, but at Goldungari and Nanikhatva, they are greenish in colour. Presence of unoriented amphibole needles (Fig.8.3a), elephant skin weathering (Fig.8.3b), rare occurrence of foliations (Fig.8.3c) and calc-silicates with greenish appearance (Fig.8.3d) are the characteristic features observed in these rocks.

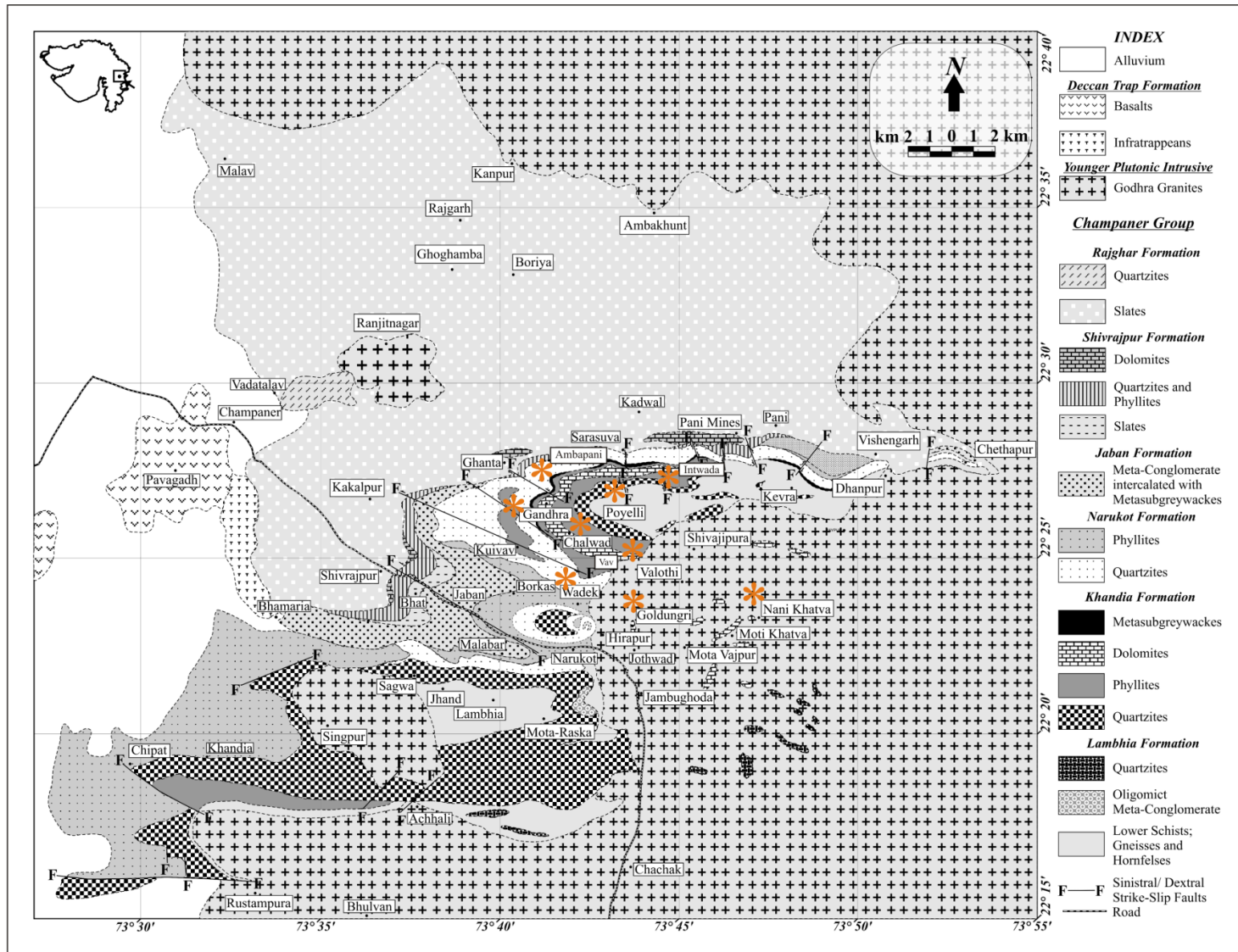


Figure 8.2: Geological map of the study area within the Champaner Group, (after Joshi, 2019). Orange coloured stars represent Calc-silicate sample locations.

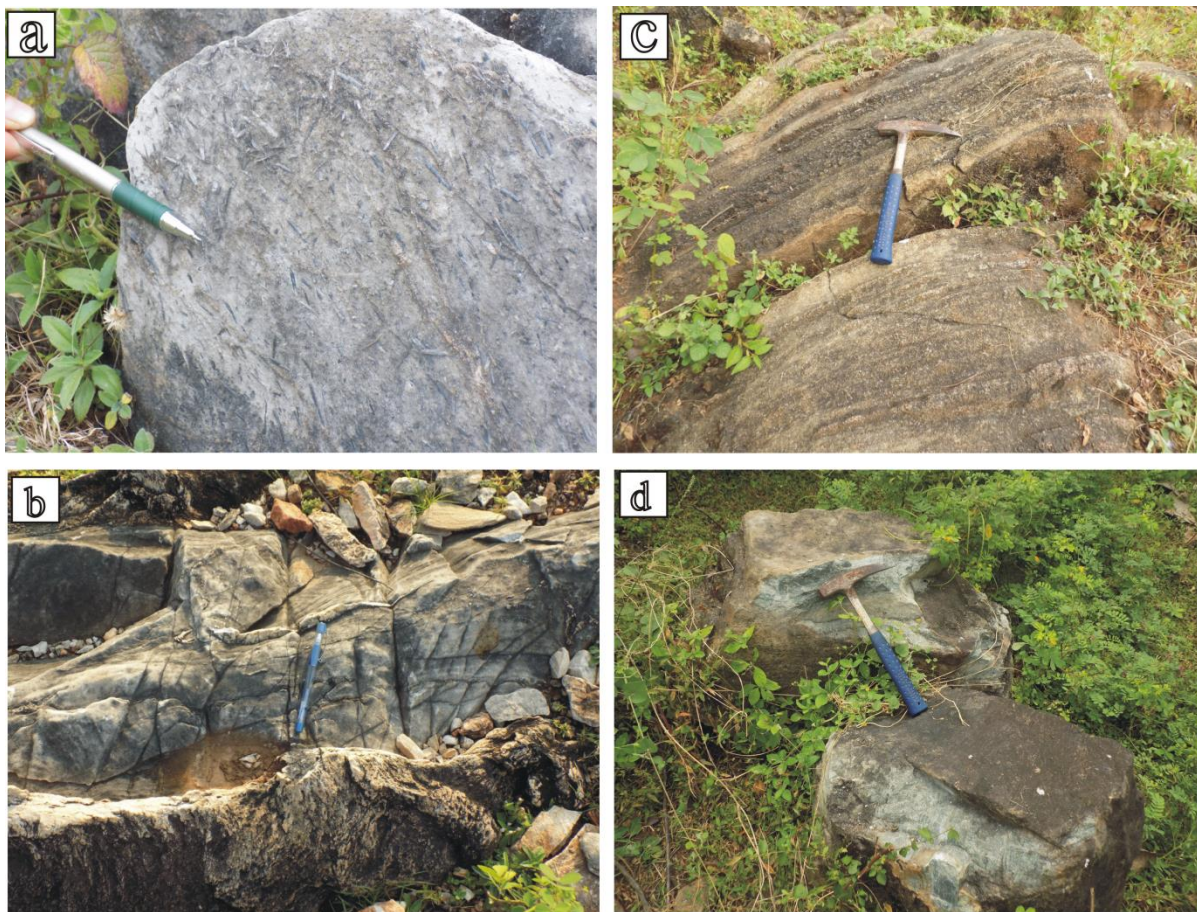


Figure 8.3: Field photograph showing, (a) Unoriented amphibole needles within calc-silicate rock, Loc. Intwada; (b) Elephant skin weathering, Loc.Chalvad; (c) Foliations, Loc. Vav; (d) Calc-silicates having greenish colour, Loc. Goldungari.

8.4 Petrography

Prominent hornfelsic texture along with the secondary porphyro-poikiloblastic texture and the granoblastic polygonal groundmass composed of dolomite, quartz and calcite are observed within these rocks. These rocks possess about 60-70 % of dolomitic matrix as compared to the calc-silicates of the study area around Lunavada which possess less than 5% volume of carbonate minerals (calcite/ankerite), hence these rocks can be termed as calc-silicate marbles or impure marbles as per the SCMR classification scheme. The mineral assemblage observed within these rocks is dolomite + tremolite + diopside + scapolite + titanite + talc + quartz ± calcite ± garnet ± chlorite ± plagioclase feldspar ± microcline along with minor proportion of opaques as compared to the assemblage, viz. actinolite + diopside + quartz + titanite + calcite ± microcline ± biotite ± plagioclase feldspar ± epidote ± scapolite ± chlorite seen within calc-silicates from Lunavada region.

Dolomite grains are distinguished by their subhedral to euhedral shape and occur as medium to fine grained aggregates. They show symmetrical extinction. Tremolites present are skeletal, acicular to diamond/pseudohexagonal in shapes having higher order colours, moderate relief, inclined extinction and are un-oriented in nature. They can be seen replacing associated dolomite, thus the reaction is,

$5\text{Dol} + 8\text{Qz} + \text{H}_2\text{O} = \text{Tr} + 3\text{Cal} + 7\text{CO}_2$ (Fig.8.4a). Subidioblastic diopsides are present and are highly cleaved having 90° angles between two sets of cleavages. High positive relief and higher interference colours are shown by diopside grains. They surround tremolites indicating the reaction of diopside formation as,



Anhedral to subhedral shaped scapolite exhibits moderate relief as well as prominent cleavages. In few samples poikiloblastic scapolites containing quartz inclusions can be seen. Scapolites are always seen in proximity to calcite indicating reaction of its formation as,

$\text{Calcite} + 3 \text{Plagioclase} = \text{Scapolite}$, but the plagioclase feldspar is not observed which suggests that it might have got consumed completely. This is a vapour absent reaction (Moecher and Essene, 1990; Satish-Kumar et al., 1995), (Fig.8.4c) Titanites are having shapes from anhedral to euhedral and possess distinct relief with higher order colours. Foliated grains of talc can be observed. They have low relief and are non-pleochroic (Fig.8.5c). Anhedral quartz grains show sharp extinction. Calcite grains are distinguished by their anhedral shape. Subhedral to euhedral garnet is present in few samples only and possesses skeletal or poikiloblastic texture (Fig.8.4c, 8.5b).

Very few samples possess chlorite and it is present in 1 to 2 % of modal amount only. Flaky crystals of chlorite show colourless to dark green pleochroism and high relief. Subhedral plagioclase feldspar and microcline also occur in few samples in negligible amount.

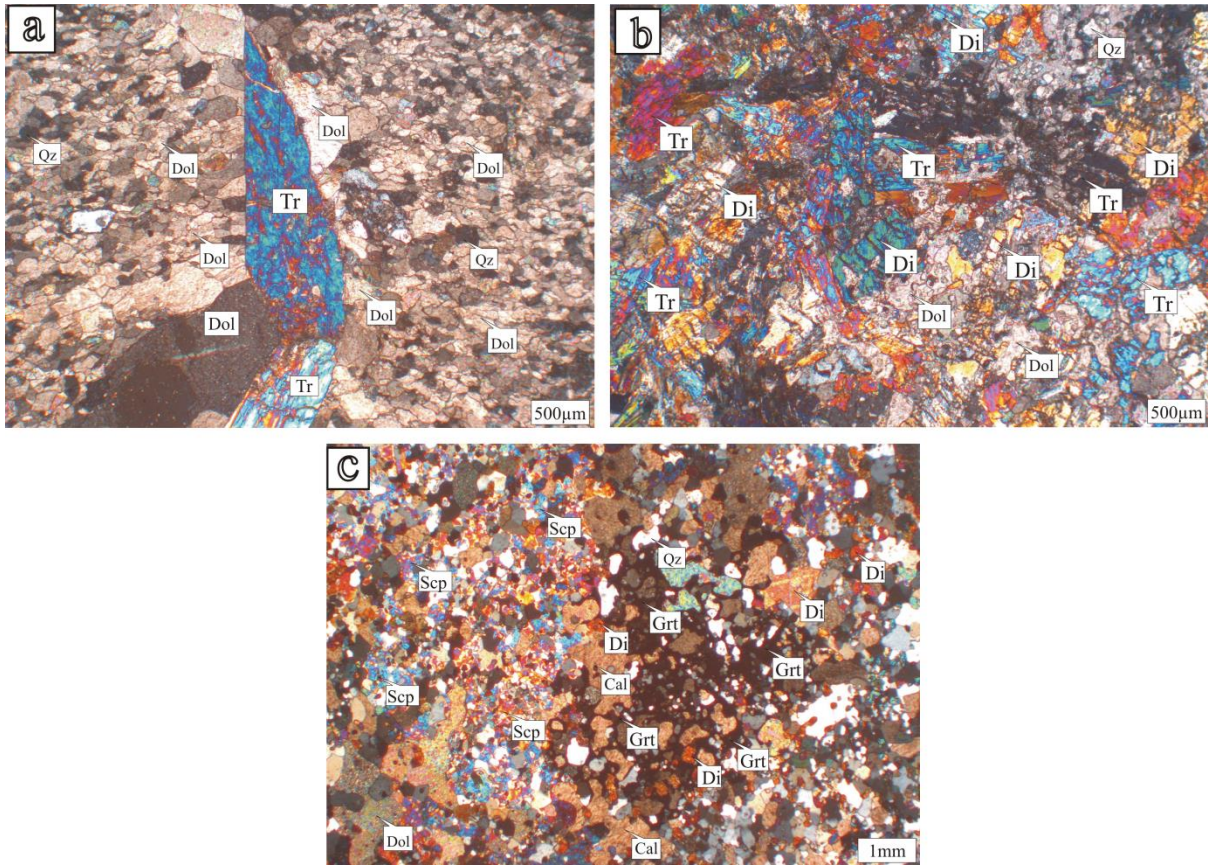


Figure 8.4: Photomicrographs (in crossed polars) of calc-silicate samples showing; (a) Formation of tremolite by replacement of dolomite; (b) Diopside nucleating along the borders of tremolite; (c) Scapolite associated with calcite and poikiloblastic garnet having quartz and calcite inclusions.

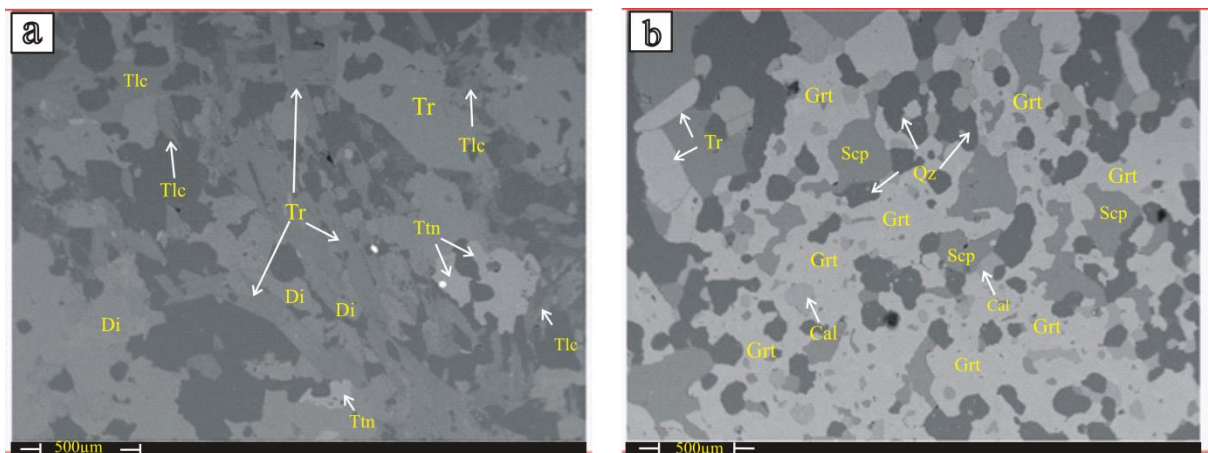


Figure 8.5: Back Scattered Electron images of major and important calc-silicate minerals and reaction textures, a) Tremolites replaced by diopside, b) Poikiloblastic garnet.

8.5 Mineral chemistry

To understand the mineral chemistry, the Electron Probe Micro Analysis (EPMA) was carried out for all important silicate mineral phases present in the calc-silicate rocks with the help of CAMECA SXFive instrument at DST-SERB National Facility, Department of Geology (Center of Advanced Study), Institute of Science, Banaras Hindu University. Mineral chemistry of important mineral phases present within the calc-silicates is discussed below:

Calcic- amphibole

Representative microprobe analyses of the calcic-amphibole are listed in the (Table 8.1) and plotted in the (Fig.8.6). All studied amphiboles can be classified as calcic amphiboles as per the nomenclature suggested by Leake (1978). The calcic amphiboles of these calc-silicates correspond to the tremolite with $(\text{Na}+\text{K})_A < 0.5$ apfu, $\text{Ti} < 0.5$ apfu (Table II, Leake et al.,1997).The tremolitic composition have 7.7 to 7.9 apfu Si, 0.06-0.39 apfu Al^{tot} , 1.94-2.1 apfu Ca and $(\text{Mg} / \text{Mg} + \text{Fe}^{2+} \text{ or } X_{\text{Mg}})$ values between 0.94-0.96.

Clino-pyroxene

Representative microprobe analyses of the clinopyroxene are listed in the (Table 8.2) and plotted in the (Fig.8.7).Clino-pyroxene (Cpx), here, is essentially a diopside-hedenbergite solid solution (Wo_{50-53} , En_{26-36} , Fs_{9-22}). The composition is mainly diopsidic as shown in Ca-Mg-Fe triangular plot with X_{Mg} ranging from 0.56-0.65. In these analyses Al is both tetrahedrally and octahedrally co-ordinated. These calc-silicates contain 1.92-1.96 apfu Si, 0.02-0.7 Al^{tot} and 0.8-1.02 apfu Ca.

Scapolite

Scapolites of these calc-silicates are Cl-absent calcic-rich meionites. The meionite component varies from 99.61 to 99.75% (Table 8.3). Analytical totals range from 98 to 99% suggesting $\text{CO}_2 + \text{H}_2\text{O}$ to be about 1 to 2%. F, Cl and SO_3 occur below detection limit.

Titanite

Titanite contains 0.94 -0.99 apfu Ca, 0.71-0.79 apfu Ti, 0.37-0.51 apfu Al. A typical titanite has the formula $\text{Ca}_{0.99} (\text{Ti}_{0.78}\text{Al}_{0.39} \text{Fe}_{0.012}) \text{Si}_{0.96} (\text{F}_{0.23})$. Sodium, Mn, K and Ba were measured in amounts 0.00-0.0016 wt % oxide concentration. Mg is below detection limit. All Fe is calculated as FeO (Table 8.3)

Talc

Most of the talc has typically near end-member compositions. Mg^{2+} is the highly dominant octahedral cation. The microprobe analyses of the talc reveal only small amounts of FeO in addition to the end member components. Fe and Al contents of talc show different compositional ranges. Near absence of Ti concentration in talc is probably due to originally poor concentration in primary carbonate phase i.e. parent material like dolomite (Table 8.4).

Garnet

The garnet exhibits an extensive grossular-spessartite-pyropite solid solution. The chemical composition of garnet shows comparatively higher grossular mole % i.e. 98.1-101%, spessartite mole % as 1.6-2.4%. Pyropite shows negligible mole % while almandine molecule is absent (Table 8.5).

Chlorite

Chemical characterisation revealed that the chlorite possesses composition ranging from sheridanite to clinocllore (Fig.8.8). Analytical data is presented in (Table 8.6).

Plagioclase Feldspar

Representative microprobe analyses of the plagioclase feldspar are listed in the (Table 8.6) and have a representative composition of $Or_{0.4}Ab_{32.0}An_{67.5}$.

A comparative study with respect to the mineral chemistry of major minerals like calcic amphibole and clino-pyroxene of the calc-silicates from the Champaner and the Lunavada regions reveals that they are different in composition. As the $Mg \gg Fe$ in amphibole of calc-silicate of Champaner, it becomes tremolitic. Whereas Mg is either slightly higher than Fe or almost 50-50% of Mg-Fe is present in the amphiboles of calc-silicates from Lunavada, due to which its chemical composition varies from magnesio-hornblende to actinolite. The clino-pyroxene of calc-silicates is totally diopsidic in case of Champaner region whereas ample amount of Fe available in Cpx of rocks from Lunavada makes them more salitic in composition. Similarly, meionite component of scapolite of Champaner ranges from 99.6 to 99.7% whereas that of Lunavada ranges from 93.7 to 99.8% and the chlorite composition of calc-silicates of Champaner ranges from sheridanite to chlorite while it shows compositional range from pycnochlorite to clinocllore in case of calc-silicates of Lunavada.

Table 8.1: Representative EPMA analyses of Calcic-amphibole

Rock No.	Chlvd- 4/3	Chlvd- 4/5	Chlvd- 4/9	Gndh- 4B/2	Gndh- 4B/3	Gndh- 4B/5
SiO ₂	56.19	56.39	57.57	57.29	57.78	57.37
TiO ₂	0.033	0.09	0.004	0.034	0.00	0.033
Al ₂ O ₃	2.42	1.62	0.80	2.053	0.39	1.23
FeO	2.50	2.38	2.27	2.096	1.93	2.15
MnO	0.087	0.17	0.11	0.072	0.17	0.072
MgO	22.14	22.74	23.19	22.70	23.35	23.54
CaO	13.85	13.14	13.92	14.20	14.31	13.45
Na ₂ O	0.10	0.09	0.01	0.10	0.035	0.036
K ₂ O	0.0027	0.00	0.00	0.00	0.00	0.00
Total	97.34	96.66	97.91	98.56	97.98	97.89
Ions on the basis of 23(O)						
Si	7.74	7.77	7.93	7.89	7.96	7.90
Ti	0.003	0.01	0.0004	0.0035	0.00	0.003
Al	0.39	0.26	0.13	0.33	0.063	0.20
Fe ⁺²	0.28	0.27	0.26	0.24	0.22	0.24
Mn	0.01	0.02	0.01	0.0085	0.020	0.0085
Mg	4.55	4.67	4.76	4.66	4.79	4.83
Ca	2.045	1.94	2.05	2.09	2.11	1.98
Na	0.027	0.02	0.004	0.027	0.009	0.009
K	0.0004	0.00	0.00	0.00	0.00	0.00
X _{Mg}	0.96	0.94	0.95	0.95	0.96	0.95

Table 8.2: Representative EPMA analyses of Clino-pyroxene

Rock no.	Vav- 3/1	Vav- 3/2	Vav- 3/5	Gldn- 17/2	Gldn- 17/4	Gldn- 17/5
SiO ₂	48.12	49.41	51.29	51.52	52.41	51.06
TiO ₂	0.032	0.035	0.00	0.019	0.035	0.015
Al ₂ O ₃	0.56	0.74	0.46	0.65	0.74	0.84
Cr ₂ O ₃	0.32	0.04	0.016	0.016	0.04	0.045
FeO	1.28	1.74	11.2	12.83	6.60	13.06
MnO	0.42	0.66	0.99	1.009	0.66	1.14
MgO	20.43	19.68	10.34	9.81	13.87	9.29
CaO	27.75	26.55	25.14	24.61	24.81	24.51
Na ₂ O	0.16	0.20	0.18	0.19	0.20	0.21
K ₂ O	0.23	0.001	0.011	0.011	0.001	0.014
Total	99.61	99.05	99.66	100.70	100.50	100.23
Ions on the basis of 6(O)						
Si	1.92	1.96	1.95	1.95	1.95	1.94
Ti	0.008	0.003	0.00	0.0005	0.0002	0.0004
Al	0.68	0.70	0.02	0.029	0.029	0.037
Cr	0.13	0.05	0.0004	0.0005	0.0008	0.0013
Fe(ii)	0.61	0.63	0.35	0.40	0.37	0.41
Mn	0.002	0.002	0.032	0.032	0.036	0.037
Mg	0.91	0.95	0.58	0.55	0.58	0.52
Ca	0.90	0.86	1.02	1.002	1.02	0.99
Na	0.07	0.09	0.013	0.014	0.014	0.015
K	0.003	0.008	0.0005	0.0005	0.00	0.0006
X _{Mg}	0.60	0.65	0.62	0.58	0.61	0.56
Pyroxene components						
Wo	53.68	51.24	50.95	49.86	50.38	50.15
En	36.14	34.36	29.18	27.67	28.78	26.47
Fs	9.08	11.65	19.17	21.75	20.13	22.56

Table 8.3: Representative EPMA analyses of Scapolite and Titanite

Scapolite					Titanite				
Rock no.	Chlvd- 4/6	Chlvd- 4/7	Gldn- 17/7	Gldn- 17/9	Rock no.	Chlvd- 4/11	Chlvd- 4/13	Gndh- 4B/9	Gndh- 4B/10
SiO ₂	41.92	42.29	42.31	42.29	SiO ₂	30.45	30.15	30.20	30.22
TiO ₂	0.00	0.00	0.01	0.00	TiO ₂	32.96	30.42	31.89	32.93
Al ₂ O ₃	35.06	35.11	34.69	35.29	Al ₂ O ₃	4.66	6.22	5.36	5.32
FeO	0.10	0.10	0.09	0.16	FeO	0.47	0.31	0.37	0.34
MnO	0.06	0.00	0.03	0.08	MgO	0.00	0.00	0.00	0.01
MgO	0.016	0.00	0.00	0.013	MnO	0.00	0.01	0.00	0.02
CaO	20.49	20.78	20.52	20.49	CaO	29.32	29.24	28.76	28.20
Na ₂ O	0.17	0.15	0.12	0.12	Na ₂ O	0.01	0.00	0.00	0.00
K ₂ O	0.00	0.00	0.00	0.02	K ₂ O	0.01	0.04	0.04	0.02
F	0.08	0.00	0.02	0.00	Cr ₂ O ₃	0.08	0.01	0.09	0.00
Cl	0.0	0.00	0.02	0.019	P ₂ O ₅	0.00	0.05	0.00	0.00
					BaO	0.00	0.00	0.00	0.00
					ZrO ₂	0.00	0.00	0.00	0.00
					Nb ₂ O ₅	0.00	0.00	0.00	0.00
					F	2.36	3.59	2.84	3.27
					Cl	0.00	0.01	0.00	0.03
Total	97.94	98.51	97.94	98.76	Total	100.32	100.05	99.55	100.36
Ions on the basis of 12(Si,Al)					Ions on the basis of 5(O)				
Si	5.97	5.98	6.03	5.99	Si	0.96	0.94	0.95	0.94
Ti	0.00	0.00	0.0008	0.00	Ti	0.78	0.71	0.75	0.77
Al	4.42	4.39	4.37	4.42	Al	0.39	0.51	0.44	0.43
Fe	0.005	0.0056	0.0051	0.0093	Fe	0.012	0.008	0.009	0.008
Mn	0.003	0.00	0.0017	0.0046	Mg	0.00	0.00	0.00	0.0004
Mg	0.0017	0.00	0.00	0.0013	Mn	0.00	0.0002	0.00	0.0005
Ca	1.56	1.57	1.56	1.55	Ca	0.99	0.97	0.97	0.94
Na	0.006	0.0051	0.0038	0.004	Na	0.0003	0.00	0.0001	0.00
K	0.00	0.00	0.00	0.0004	K	0.0004	0.0015	0.0016	0.0007
F	0.018	0.00	0.0042	0.00	P	0.00	0.004	0.0008	0.00
Cl	0.00	0.00	0.0025	0.0021	Ba	0.00	0.00	0.00	0.00
					Zr	0.00	0.00	0.00	0.00
Mol%	99.61	99.67	99.75	99.71	Nb	0.00	0.00	0.00	0.00
Meionite					F	0.23	0.35	0.28	0.32
					Cl	0.00	0.0005	0.0001	0.001

Table 8.4: Representative EPMA analyses of Talc

Rock no.	Chlvd-4/20	Chlvd-4/22	Gldn-17/30	Gldn-17/31
SiO ₂	62.15	62.73	61.75	62.34
Al ₂ O ₃	0.649	0.366	0.404	0.573
FeO	2.045	2.133	1.837	1.718
MgO	29.99	30.47	30.59	30.66
MnO	0.029	0.102	0.102	0.029
CaO	0.056	0.020	0.035	0.088
Na ₂ O	0.056	0.039	0.045	0.075
Total	94.97	95.86	94.76	95.48
Ions on the basis of 22(O)				
Si	7.22	7.23	7.18	7.16
Al	0.06	0.03	0.041	0.058
Fe	0.09	0.1	0.08	0.08
Mg	5.2	5.25	5.34	5.29
Mn	0.001	0.004	0.005	0.001
Ca	0.003	0.001	0.002	0.005
Na	0.0015	0.001	0.001	0.02

Table 8.5: Representative EPMA analyses of Garnet

Rock no.	Gldn- 17/7	Gldn- 17/8	Gldn- 17/9	Gldn- 17/10	Gldn- 17/11	Gldn- 17/12
SiO ₂	36.21	37.08	36.83	36.84	36.80	36.63
TiO ₂	0.70	0.709	0.68	0.70	0.63	0.75
Al ₂ O ₃	9.08	11.84	10.62	11.20	11.69	9.57
Cr ₂ O ₃	0.052	0.031	0.014	0.045	0.062	0.018
Fe ₂ O ₃	0.00	0.00	0.00	0.00	0.00	0.00
FeO	16.90	12.64	14.52	14.13	13.27	15.51
MnO	0.71	0.96	0.86	0.85	1.08	0.86
MgO	0.00	0.096	0.072	0.059	0.08	0.040
CaO	34.65	34.74	34.77	34.22	34.57	34.26
Total	98.33	98.11	98.39	98.07	98.20	97.67
Ions on the basis of 24 (O)						
Si	5.83	5.91	5.88	5.89	5.87	5.92
Ti	0.085	0.085	0.082	0.085	0.075	0.09
Al	1.29	1.66	1.501	1.58	1.64	1.36
Cr	0.005	0.0029	0.0013	0.0043	0.0059	0.0017
Fe ³⁺	0.00	0.00	0.00	0.00	0.00	0.00
Fe ²⁺	1.13	0.84	0.97	0.94	0.88	1.048
Mn	0.048	0.064	0.058	0.057	0.072	0.059
Mg	0.00	0.011	0.0086	0.007	0.009	0.0048
Ca	2.98	2.96	2.97	2.93	2.95	2.96
Almandine mole %	-2.67	-1.48	-1.99	-0.27	-2.17	-0.82
Pyrope mole %	0.00	0.38	0.288	0.23	0.33	0.16
Grossularite mole %	101.03	98.94	99.74	98.10	99.38	98.69
Spessartite mole %	1.64	2.16	1.96	1.93	2.45	1.96

Table 8.6: Representative EPMA analyses of chlorite and plagioclase feldspar

Chlorite				Plagioclase feldspar			
Rock no.	Gndh-9A/5	Gndh-9A/6	Gndh-9A/8	Rock no.	Gldn-17/15	Gldn-17/16	Gldn-17/20
SiO ₂	28.89	28.91	29.95	SiO ₂	52.41	51.76	52.77
TiO ₂	0.041	0.063	0.027	Al ₂ O ₃	25.79	27.53	26.25
Al ₂ O ₃	21.66	21.86	20.98	FeO	0.000	0.10	0.010
Cr ₂ O ₃	0.00	0.031	0.006	CaO	16.94	16.14	15.61
Fe ₂ O ₃	0.78	0.73	0.64	Na ₂ O	3.4	4.23	4.6
FeO	3.86	3.69	3.38	K ₂ O	0.55	0.08	0.1
MnO	0.063	0.00	0.00	BaO	0.00	0.00	0.00
MgO	29.29	29.86	31.57				
NiO	0.033	0.11	0.00				
CaO	0.048	0.066	0.037				
Na ₂ O	0.00	0.008	0.0041				
K ₂ O	0.024	0.032	0				
F	0.00	0.10	0.24				
Cl	0.0023	0.037	0.013				
H ₂ O*	12.31	12.29	12.39				
Total	97.03	97.8	99.28	Total	99.09	99.84	99.34
O=F,Cl	0.0005	0.054	0.106				
TOTAL	97.03	97.78	99.17				
Ions on the basis of 28(O)				Ions on the basis of 32(O)			
Si	5.61	5.55	5.64	Si	9.73	9.535	9.75
Al iv	2.38	2.44	2.35	Al	5.64	5.977	5.71
Al vi	2.58	2.52	2.32	Fe(ii)	0.00	0.015	0.002
Ti	0.006	0.009	0.0039	Ca	3.37	3.185	3.09
Cr	0.00	0.004	0.0008	Na	1.22	1.511	1.64
Fe ³⁺	0.11	0.106	0.091	K	0.13	0.019	0.02
Fe ²⁺	0.62	0.59	0.53	Ba	0.00	0.000	0.00
Mn	0.01	0.00	0.00				
Mg	8.48	8.55	8.87	Feldspar components			
Ni	0.0052	0.018	0.00	An	71.33	67.56	64.90
Ca	0.01	0.013	0.00	Ab	25.91	32.04	34.61
Na	0.00	0.006	0.007	Or	2.76	0.40	0.50
K	0.012	0.015	0.002				
Rb	0.00	0.00	0.00				
F	0.00	0.13	0.29				
Cl	0.0015	0.02	0.008				
OH*	15.99	15.84	15.69				
X _{Mg}	0.93	0.94	0.94				

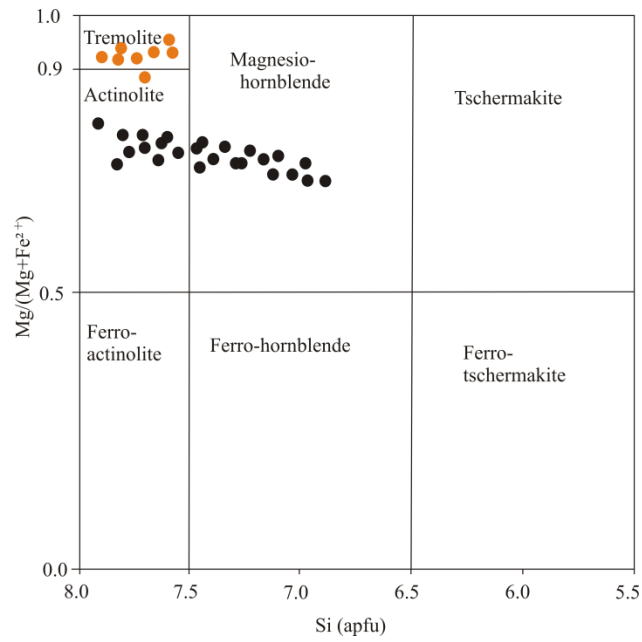


Figure 8.6: Calcic-amphibole, classification scheme after Leake et al.,(1997). (Orange solid circles indicate samples from Champaner region and black solid circles represent samples from Lunavada region)

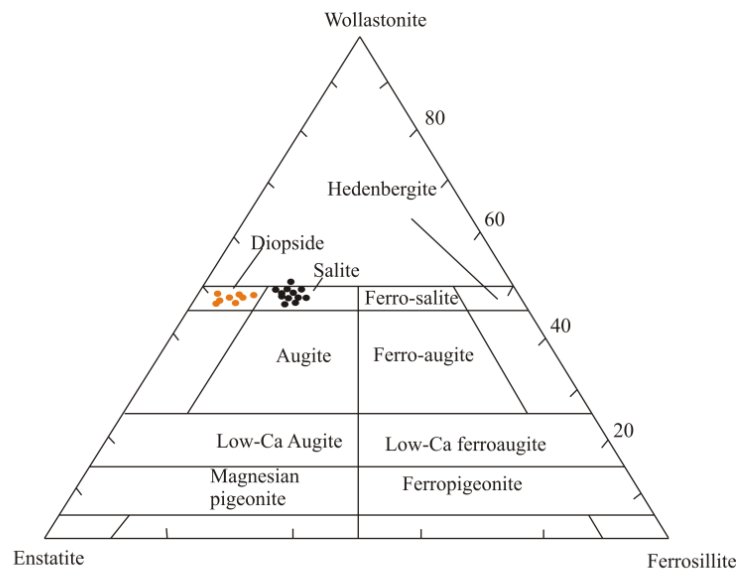


Figure 8.7: Ca-Mg-Fe triangular plot showing Clinopyroxene composition.

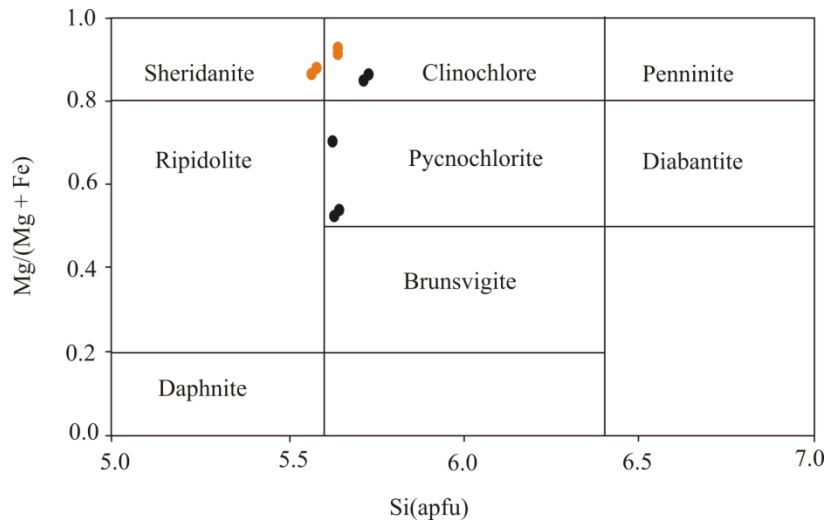


Figure 8.8: Nomenclature and classification of Chlorite (after Hey,1954).

8.6 Geochemistry

Seven representative samples of the calc-silicate rocks of study area were analysed for determining major oxide, trace as well as rare earth elements (REEs) concentration. Major oxide data acquired using Wavelength Dispersive X-Ray Fluorescence (WD-XRF) using Philips MagiX PRO model PW 2440 wavelength dispersive X-ray fluorescence spectrometer coupled with automatic sample changer PW 2540, while trace elements and REEs have been analysed using High Resolution Inductively Coupled Plasma Mass Spectrometer (HR-ICP-MS; Nu Instruments Attom, UK) at the CSIR National Geophysical Research Institute, Hyderabad, following acid digestion that involves repeated treatment with HF-HNO₃-HClO₄. JLS-1, JG-2 and MRG1 were used as standards. Analytical results for major, trace and rare-earth elements are presented in Table 8.7.

8.6.1 Major, trace and rare-earth elements compositions

Analysed calc-silicate rocks exhibit a range of SiO₂ (15.7-36.9 wt.%), Al₂O₃ (0.5-3.6 wt.%) FeO (0.6-2.6 wt.%) and MnO (0.03-0.19 wt.%) which is lower than the average composition of post-archean upper continental crust (PAUCC) of Taylor and McLennan (1985) whereas MgO (2.1-13.2 wt.%) and CaO (22.1-33.9 wt.%) whole-rock compositions show enrichment relative to the compositions of PAUCC.

Table 8.7: Major (wt%), trace and rare earth element (ppm) analyses of the representative calc-silicate rock samples

Sample No.	Gndh-11	Gndh-06	Gndh-9A	Intwd-16	Gldn-17	Vav-03	Gndh-4B
SiO ₂	18.59	20.80	22.18	17.26	36.93	19.09	15.78
Al ₂ O ₃	1.50	1.03	1.69	0.74	3.63	0.71	0.53
FeO	1.62	2.64	2.1	0.64	1.94	1.66	0.72
MnO	0.12	0.19	0.08	0.03	0.14	0.15	0.07
MgO	13.20	12.85	12.78	13.24	2.11	13.26	13.25
CaO	23.45	24.47	25.23	22.10	33.96	23.86	24.35
Na ₂ O	0.10	0.07	0.13	0.10	0.51	0.11	0.07
K ₂ O	0.03	0.01	0.03	0.03	1.42	0.04	0.13
TiO ₂	0.05	0.03	0.08	0.03	0.15	0.03	0.02
P ₂ O ₅	0.08	0.07	0.13	0.03	0.68	0.08	0.09
LOI	40.29	37.57	35.73	45.08	17.08	41.24	45.83
Sc	3.346	3.297	4.404	2.040	10.592	2.037	1.780
V	18.898	19.693	19.983	12.710	25.904	21.544	15.417
Cr	52.936	94.064	137.580	42.136	139.016	114.739	31.577
Co	3.967	7.906	8.057	4.338	13.722	7.915	2.633
Ni	82.256	97.774	97.481	47.681	94.754	116.900	41.888
Cu	42.956	54.024	55.126	39.655	57.080	109.410	37.802
Zn	94.008	130.904	139.760	107.586	151.092	197.938	81.652
Ga	2.257	2.263	3.615	0.983	8.424	1.511	0.999
Rb	2.338	2.352	2.976	2.353	89.266	3.050	7.802
Sr	54.063	79.249	64.816	45.412	766.359	76.412	54.607
Y	3.888	4.644	6.089	2.482	36.471	3.010	1.969
Zr	34.144	27.862	48.888	22.986	61.041	23.470	19.172
Nb	1.697	1.108	2.783	0.920	6.013	0.888	0.534
C	0.323	0.101	0.217	0.131	2.421	0.140	0.395
Ba	25.322	29.836	27.225	18.844	1753.95	31.879	23.163
La	4.322	7.858	6.628	3.371	47.608	4.036	1.532
Ce	8.469	14.814	13.098	6.400	91.561	7.650	3.071
Pr	1.018	1.674	1.565	0.774	10.738	0.898	0.378
Nd	3.772	5.872	5.947	2.746	38.727	3.536	1.496
Sm	0.772	1.054	1.284	0.508	7.454	0.817	0.348
Eu	0.189	0.326	0.298	0.136	1.801	0.221	0.091
Gd	0.704	0.886	1.166	0.439	6.990	0.719	0.364
Tb	0.113	0.140	0.182	0.072	1.090	0.105	0.057
Dy	0.664	0.790	1.026	0.433	6.093	0.532	0.326
Ho	0.133	0.159	0.211	0.083	1.273	0.099	0.069
Er	0.341	0.389	0.530	0.203	3.114	0.252	0.187
Tm	0.046	0.049	0.070	0.026	0.394	0.034	0.027
Yb	0.267	0.338	0.458	0.166	2.640	0.182	0.157
Lu	0.039	0.049	0.067	0.024	0.383	0.026	0.023
Hf	0.869	0.693	1.184	0.592	1.676	0.608	0.476
Ta	0.204	0.109	0.224	0.168	0.402	0.107	0.067

Pb	4.719	16.642	12.063	6.523	10.095	22.310	6.547
Th	1.797	1.701	2.639	0.992	11.063	1.318	0.903
U	0.416	0.330	0.682	0.394	1.312	0.577	0.967
(La/Sm) ^N	3.62	4.82	3.34	4.35	4.12	3.21	2.9
(Gd/Yb) ^N	2.18	2.18	2.1	2.15	2.19	3.29	1.98
(La/Yb) ^N	11.61	16.72	10.38	14.64	12.94	16.19	7.32
Eu/Eu*	0.74	1.01	0.72	0.86	0.76	1.43	0.78
Zr/Sc	10.22	8.46	11.1	11.26	5.76	11.7	10.76
Th/Sc	0.53	0.51	0.59	0.45	1.04	0.64	0.5
Th/Co	0.45	0.21	0.32	0.22	0.8	0.16	0.34
La/Th	2.41	4.58	2.51	3.4	4.3	3.1	1.6
La/Sc	1.29	2.38	1.5	1.65	4.49	1.98	0.85
Cr/Th	29.56	55.33	52.31	42.55	12.56	87.58	35.07

The Harker plots show positive correlation of SiO₂ with Al₂O₃, Na₂O, K₂O, TiO₂, CaO, FeO and MnO whereas negative correlation with MgO only (Fig.8.9) in contrast to the calc-silicates of Lunavada wherein SiO₂ is positively correlated with Al₂O₃, Na₂O, K₂O and TiO₂ while inversely correlated with CaO, MgO, FeO and MnO.

Analysed calc-silicates show higher concentrations of Zn (81-197 ppm), Ni (41.8-116.9 ppm) and Cu (37.8-109.4 ppm) whereas lower concentrations of Ga (0.9-8.4 ppm), V (12.7-25.9 ppm), Cr (31-139 ppm) and Co (2.6-13.7 ppm) compared to PAUCC. Large-ion-lithophile elements (LILEs) viz. Rb (2.3-89.2 ppm), Ba (18-1793 ppm), Sr (45.4-766.3 ppm), Pb (4.7-22.3 ppm), U (0.3-1.3 ppm) and Th (0.9-11 ppm) show concentrations similar to PAUCC while high field strength elements (HFSEs) viz. Zr (19.1-61.0 ppm), Nb (0.5-6.0 ppm), Hf (0.4-1.6 ppm) and Ta (0.06-0.2 ppm) have concentrations lower than PAUCC.

Almost all these rocks exhibit LREE-enriched but HREE-depleted subparallel chondrite-normalized REE patterns with slight negative Eu anomalies (Eu/Eu*) ranging from 0.7 to 0.9 (Fig.8.10) in contrast to the rock samples of Lunavada which show moderately negative Eu anomalies, ranging from 0.5 to 0.7. The upper continental crust composition and post-archean sedimentary protolith is indicated by negative Eu anomaly (Taylor and McLennan, 1985). These rocks reveal fractionated REE patterns ($La^N/Yb^N = 7.3$ to 25.3) with higher total REE abundances, i.e. up to 354 ppm.

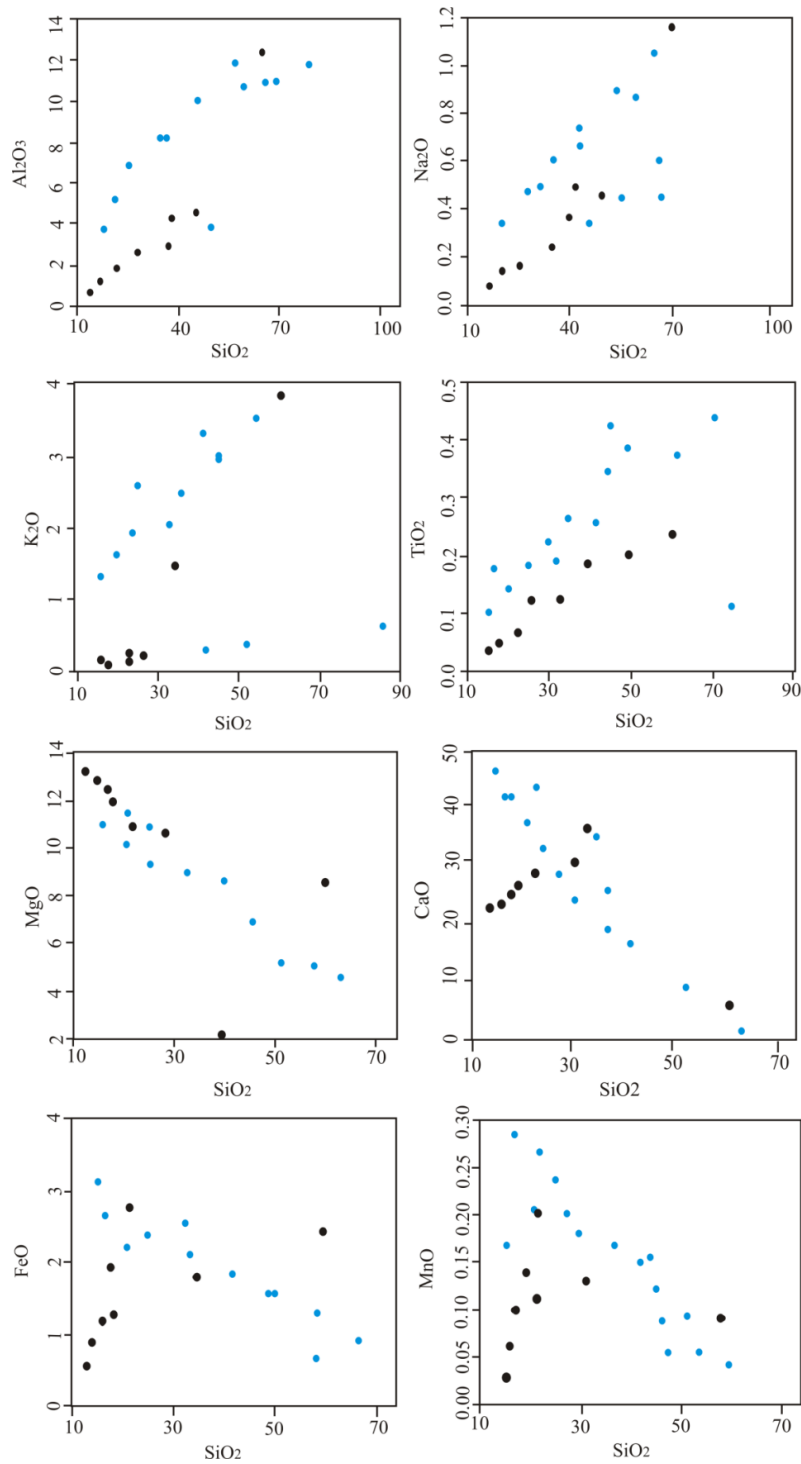


Figure 8.9: Whole-rock concentrations of major-element versus silica in weight percent oxides for calc-silicates samples. (Black solid circles represent calc-silicate rocks from Champaner region while blue solid circles denote calc-silicates from Lunavada region.) *All iron is reported as FeO.

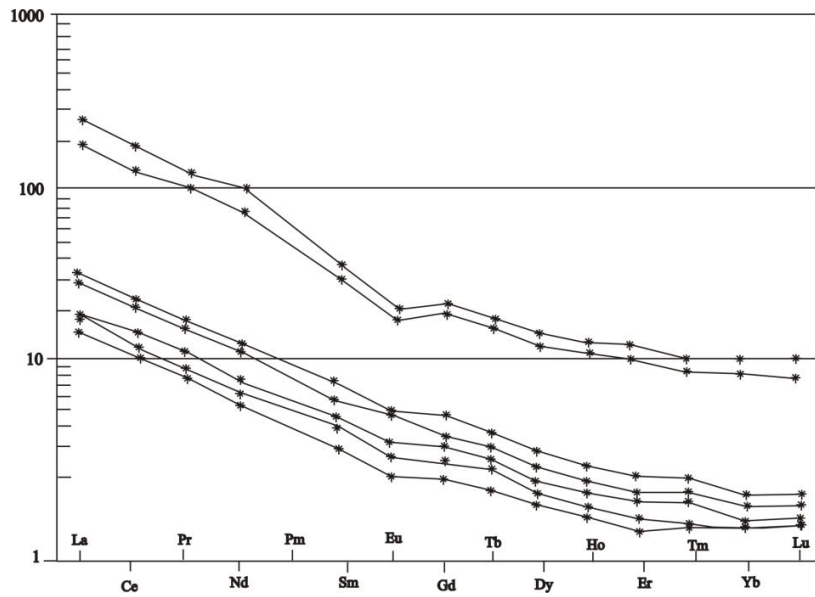


Figure 8.10: Chondrites normalized rare earth element (REE) patterns for calc-silicates of the study area within Champaner Group (after Sun and McDonough, 1989).

8.6.2 Protolith of calc-silicate rocks

Unlike calc-silicate samples of Lunavada which fall within or very near to greywacke zone on CaO, Al₂O₃ and FeO +MgO ternary diagram, the calc-silicate bulk-rock compositions of Champaner region correspond closely to the carbonates when normalized to CaO, Al₂O₃, and FeO + MgO (Fig 8.11).

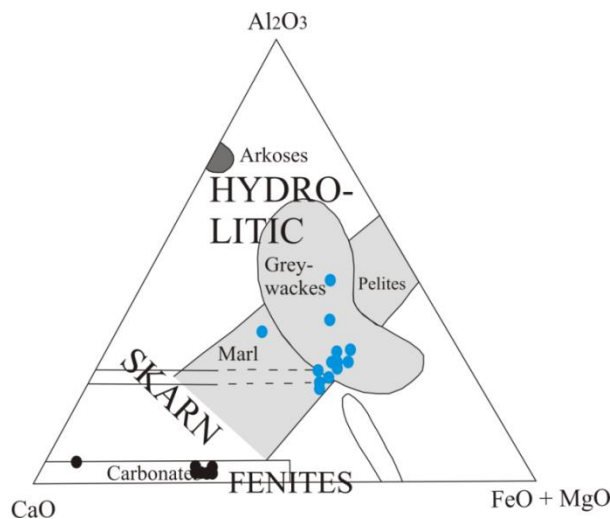


Figure 8.11: The bulk-rock compositions of calc-silicates are plotted on a CaO-Al₂O₃-FeO+MgO (wt.%) ternary diagram. General bulk compositions of unaltered arkoses, pelites, greywackes and marls are represented by shaded fields along with schematic regions for metamorphic types (after Barton et al., 1991).

The rock samples of Champaner also exhibit positive correlation between Al_2O_3 and nearly all measured trace elements along with Na_2O and K_2O similar to the Lunavada rock samples. This shows the control of K-bearing minerals or clay minerals over these trace elements. (Fig.8.12), thus suggesting that the protolith bears some clays (McLennan et al., 1990; Condie et al., 2001)

Similarly, in the study area within the Champaner Group also, the quartzite-metapelite sequence is seen. This point towards the sedimentary facies transitions from shallow-water shelf deposits to deep-water slope deposits. As the calc-silicate samples fall closer to sandstone zone on a sandstone-shale continuum of the Al-Zr-Ti diagram (Fig.8.13) of Garcia et al.,(1994), a shallow-water shelf depositional environment is indicated for primary sediments. In a CaO-MgO-SiO₂ ternary diagram classification system for marbles (Storey and Vos,1981), (Fig.8.14), most of the studied samples fall within the transition zone,i.e. from siliceous to calc-silicate marble.

All these above observations indicate that the protolith of calc-silicates from champaner area must be siliceous dolomites i.e. dolomites having quartzo-felspathic and clayey impurities.

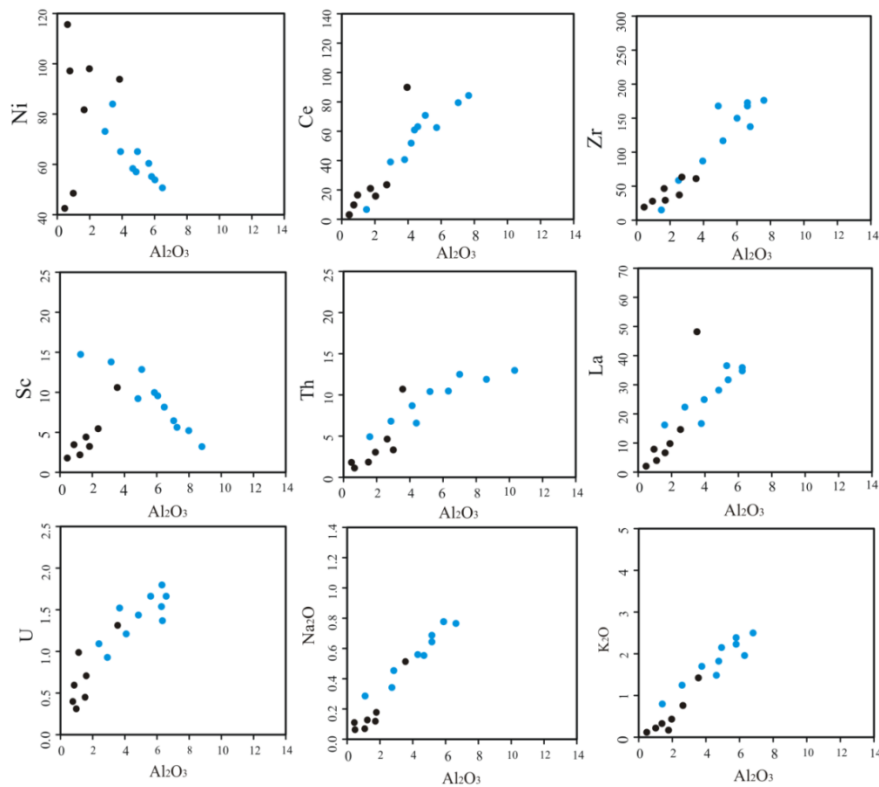


Figure 8.12: Whole-rock compositions of selected trace-elements along with Na_2O and K_2O exhibit a positive correlation with Al_2O_3 in these calc-silicates suggesting these components were bound in clays.

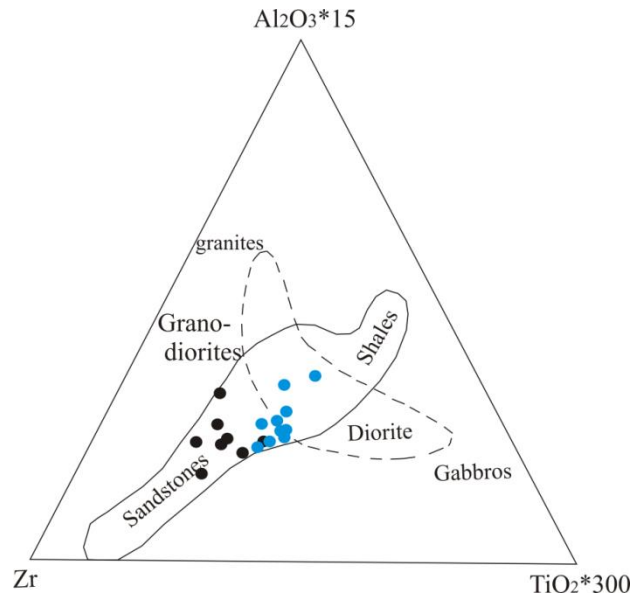


Figure 8.13: Whole-rock compositions of calc-silicates fall within the continuum between sandstone and shale (grey) on a ternary Al-Zr-Ti diagram (after Garcia et al.,1994).The field outlined by the dashed line represents the typical curved trend exhibited in whole-rock compositions of rocks derived from calc-alkaline plutonic suites.

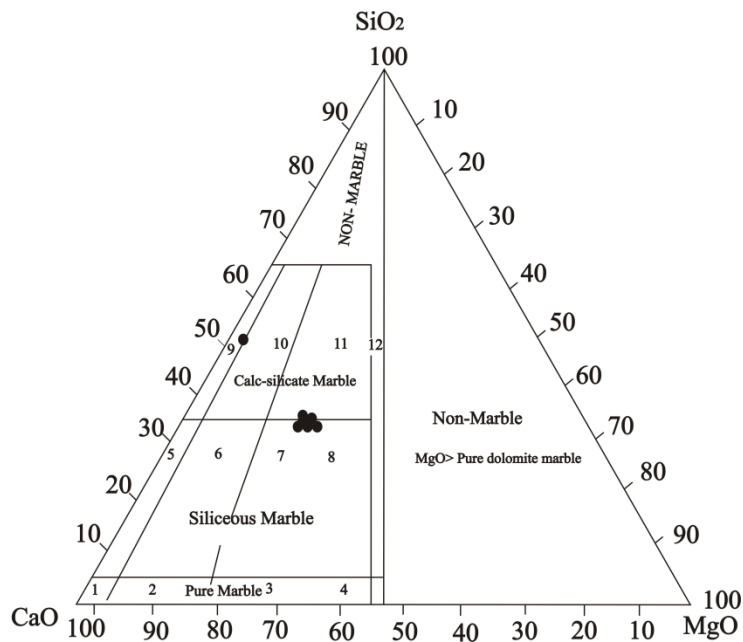


Figure 8.14: CaO-MgO-SiO₂ ternary diagram classification system for marbles,(Storey and Vos,1981).

8.6.3 Provenance and tectonic setting

Th/Sc ratio, here, is less than 0.79 suggesting a provenance from a mafic source and sediment recycling is not so high as is reflected by little zircon concentration (Fig.8.15), whereas the Th/Sc ratio > 0.79 is shown by calc-silicates of Lunavada and sediment recycling is also good as shown by higher Zr/Sc ratio than Champaner rocks.

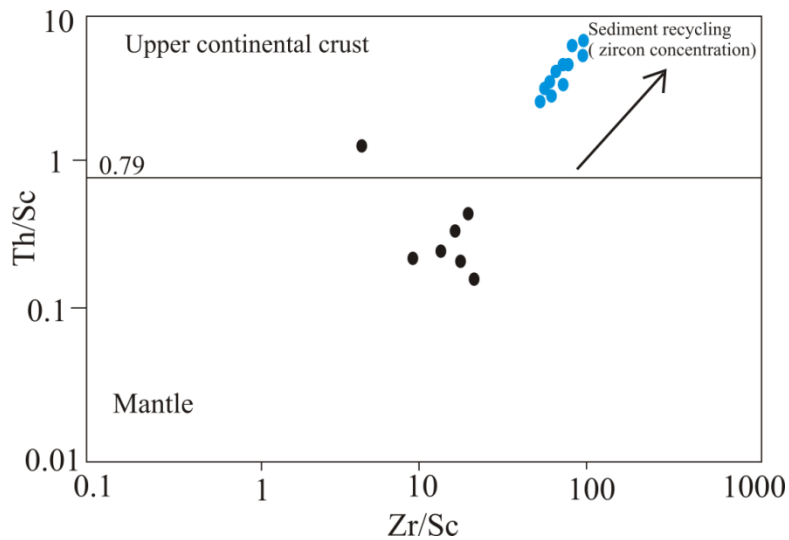


Figure 8.15 : Th/Sc vs Zr/Sc ratio diagram showing the composition of the sources for the primary sediments of calc-silicate rocks and the extent of recycling or concentration of Zr in sediments, associated with the abundance of heavy minerals, particularly zircon (after McLennan et al., 1990).

Here, it has been observed that the calc-silicate rocks of the study area of Champaner show enrichment in the incompatible elements viz. Sc, Cr and Co and are depleted in Th, Zr and La, thus emphasizing the mafic nature of provenance, as according to (Ahmad et al., 2016), detritus derived from a mafic source tend to be enriched in compatible elements like Sc, Cr and Co while those derived from a felsic source are enriched in incompatible elements like Th, Zr and La.

Calc-silicate samples fall in an array indicative of mafic composition of the source rocks in Th/Co vs. La/Sc bivariate plot in contrast to the Lunavada calc-silicates which fall in array of felsic rocks (Fig.8.16), (Cullers, 2002). Trace element studies revealed that the source of these calc-silicates was similar in composition to the average post-archean upper continental crust, maybe gabbroic/basaltic thus supporting an idea that a significant

amount of differentiated mafic igneous rocks probably present in the source area at the onset of sedimentation.

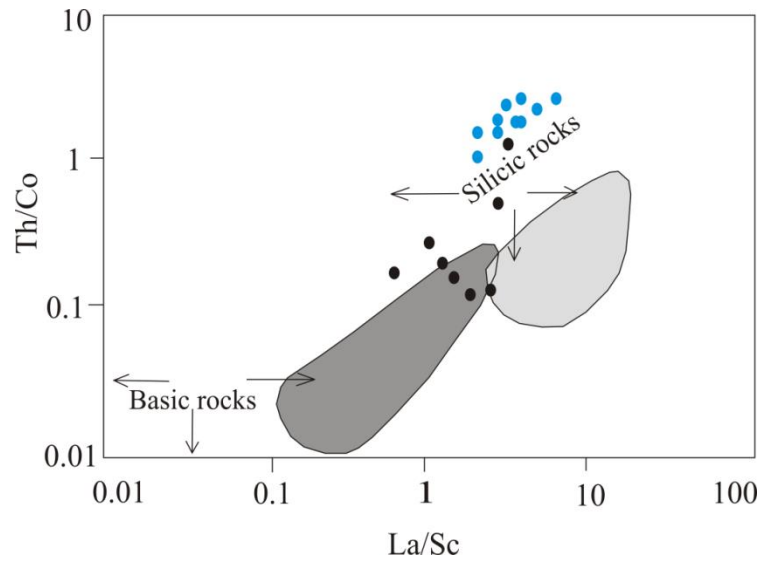


Figure 8.16: Th/Co vs. La/Sc diagram (after Cullers, 2002) where samples can be seen to be showing affinity for source rocks.

The Sc- Th- Zr/10 plot of Bhatia and Crook (1986) shows that the sample data are plotted within the field ranging from continental island arc to active continental margin settings (Fig.8.17), indicating multiple sources /provenance for these calc-silicates.

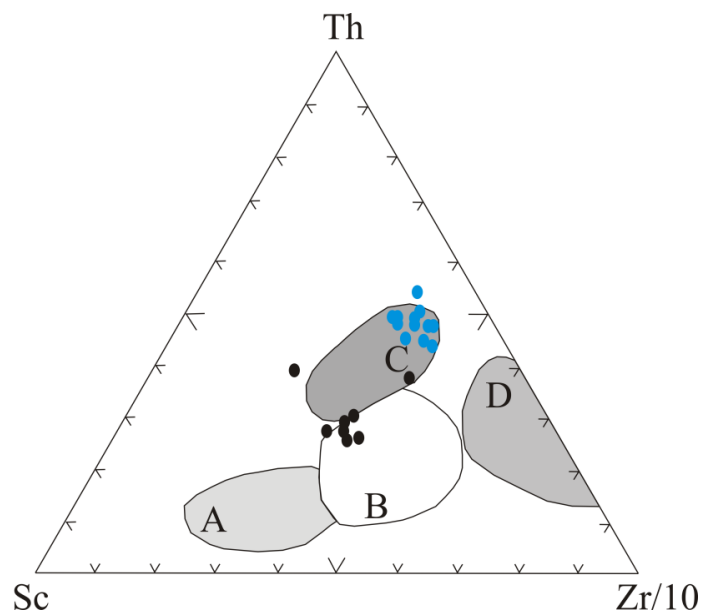


Figure 8.17: Sc-Th-Zr/10 diagram of Bhatia and Crook (1986). A: oceanic island arc; B: continental island arc; C: active continental margin D: passive/rifted margins.

8.7 Pressure and temperature conditions of calc-silicate rocks

According to Butcher and Grapes (2011), standard 1kbar pressure is estimated for the rocks within contact aureoles. Hence the pressure at peak metamorphism for the calc-silicates of the Champaner region is also considered as 1kbar, as these calc-silicates reside within well-defined contact aureole within study area. Similarly, as the suitable geothermometer is not available, it is assumed from petrographic studies that the temperature at peak metamorphism must be ranging from around 650°C to 700 °C.

8.7.1 Phase diagram/ pseudosection

Phase diagrams were constructed with the help Perple_X version 6.8.1 (Connolly, 2005; Connolly, 2009). The Holland and Powell dataset (1998), updated in 2003, was employed for end-member calculations. The solution models were employed, viz. Holland and Powell (1996) for clinopyroxene, Wei and Powell (2003) and White et al., (2003) for calcic-amphibole, Newton et al.,(1980) for plagioclase, and Waldbaum and Thompson (1968) for potassium-feldspar. Pseudosections were modelled in the system: K₂O-Na₂O-CaO-MgO-FeO-TiO₂-Al₂O₃-SiO₂-H₂O-CO₂ (KNCFMASTCH). Isobaric T-X (CO₂) pseudosections were calculated at 1kbar of pressure assuming stability of a binary H₂O-CO₂ fluid. Phase equilibrium calculations involving binary H₂O-CO₂ fluids were performed using the CORK equation of state from Holland and Powell (1991).

Pseudosection for a sample Gndh-06 is constructed for a temperature range of 300-700°C. Fluid composition range assumed between 0 and 1 for X(CO₂). Using whole rock geochemistry the equilibrium assemblage, dol+ tr +di + scp + ttn + tlc +qz + mc which was observed in thin-section of (Gndh-06) sample, used in pseudosection calculations. In the pseudosection (Fig.8.18), calcic amphibole, cpx and titanite are in equilibrium within the assemblage observed as 'amph cpx fo ttn phl nph cal ' which derived the stability field with temperature range of 610°-680°C and fluid compositions of X(CO₂) < 0.95. Carbonate-bearing zones represented as low variance fields become ubiquitous at wide range of temperature i.e. ~300-420 °C and all fluid compositions of X(CO₂) with calcite, ankerite and dolomite representing a part of protolith composition. Calcic amphibole (actinolite) appears at almost 340°C and destabilizes above 450°C with the appearance of cpx (diopside) which defines the minimum temperature required for its formation and at X(CO₂) range > 0.8. Titanite is stable at wide temperature range i.e. from 450-700°C and at all X(CO₂) compositions.

Talc is stable from 300-380°C and $X(\text{CO}_2) < 0.6$. K-feldspar is stable till 490°C and at almost all fluid compositions. Above almost 440°C, quartz destabilizes, hence does not appear in any assemblage.

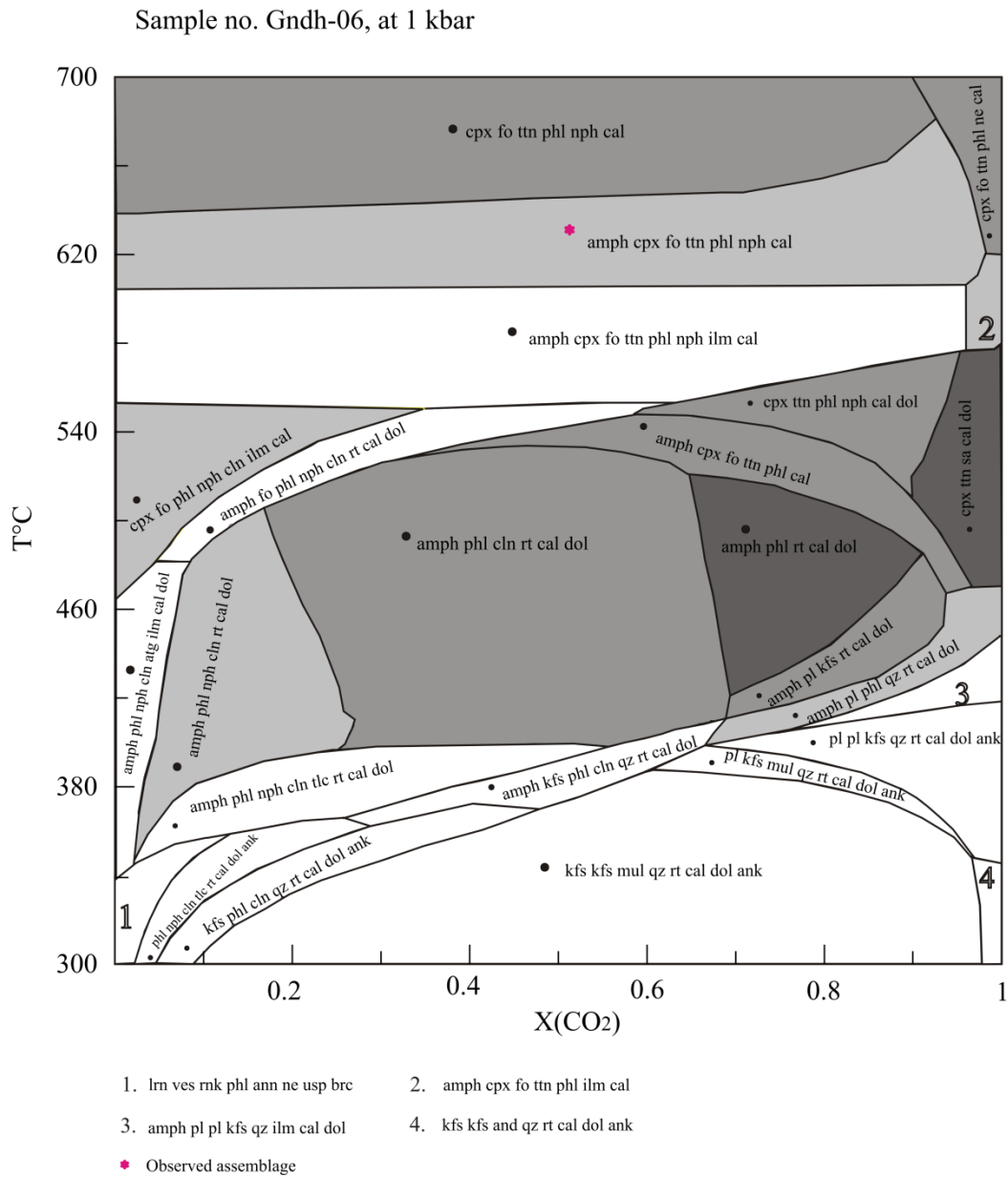


Figure 8.18: Isobaric T-X(CO₂) diagram for sample Gndh-06 at 1 kbar.

The assumed pressure and temperature at peak metamorphism of the calc-silicates of Champaner indicate metamorphic facies as 'Pyroxene-hornfels facies' of contact metamorphism. It is supported by a phase diagram or a pseudosection constructed above also, as the assemblage observed within a rock is having a stability field within a temperature range of 610°-680°C.

----- END -----